

Article

Factors Influencing the Spatio–Temporal Variability of Aerosol Optical Depth over the Arid Region of Northwest China

Fei Zhang 

College of Geography and Environmental Sciences, Zhejiang Normal University, Jinhua 321004, China; zhangfei3s@xju.edu.cn

Abstract: Aerosol optical depth (AOD) is an important physical variable used to characterize atmospheric turbidity for the management and control of air pollution. This study aims to analyze the factors influencing the spatial and temporal variability in AOD across the arid region of Northwest China (ARNC) using MODIS Aqua C006 aerosol product data from 2008 to 2017. In terms of natural and socioeconomic factors, the correlation coefficient (R) was used to identify the most influential factor in the AOD changes. The results show that AOD values in spring and summer were much higher than those in autumn and winter, especially in spring. In general, AOD had an insignificant decreasing trend, with a small overall changing range. Spatial analysis revealed a significantly decreasing trend, mostly across the Gobi Desert area, which is located in the western region of the ARNC. From the perspective of natural factors, AOD was positively correlated with air temperature (AT), wind speed (WP), land surface temperature (LST), and the digital elevation model (DEM) and negatively correlated with precipitation, relative humidity (RH), and the normalized difference vegetation index (NDVI). The greatest positive correlation, with a maximum R value of 0.8, was found between AOD and wind speed. By contrast, AOD and relative humidity had the strongest negative correlation, with R values of -0.77 . In terms of anthropogenic factors, gross domestic product (GDP), secondary industry, and population density were the three major anthropogenic factors that influenced the changes in AOD changes in this region. In general, the effects of anthropogenic factors on AOD are more significant in areas with high urban population densities.



Citation: Zhang, F. Factors Influencing the Spatio–Temporal Variability of Aerosol Optical Depth over the Arid Region of Northwest China. *Atmosphere* **2024**, *15*, 54. <https://doi.org/10.3390/atmos15010054>

Academic Editors: Haoran Liu, Wei Tan and Wenjing Su

Received: 15 October 2023
Revised: 26 December 2023
Accepted: 28 December 2023
Published: 30 December 2023



Copyright: © 2023 by the author. Licensee MDPI, Basel, Switzerland. This article is an open access article distributed under the terms and conditions of the Creative Commons Attribution (CC BY) license (<https://creativecommons.org/licenses/by/4.0/>).

Keywords: aerosol optical depth (AOD); arid region of Northwest China (ARNC); spatio–temporal variability; natural influencing factors; anthropogenic influencing factors

1. Introduction

An aerosol is a suspension of small solid–liquid particles in the air that can be divided into anthropogenic and natural sources [1–4]. Artificial aerosols are mainly produced from petroleum and chemical fuels, while natural aerosols are caused by the combustion of minerals, biomass, and blown sand and dust [5–10]. Aerosols can reduce the amount of solar radiation reaching the ground surface by absorbing and dispersing solar radiation, thus lowering ground surface temperatures and evapotranspiration rates. A high aerosol load in the atmosphere can lead to a humid micro-climate, affecting the balance of the terrestrial ecosystem [11–14] and overall Earth radiation [15–17]. The number and optical properties of clouds are influenced by aerosol concentrations, which have an impact on regional precipitation and the water cycle [18].

Northwest China is located inland on the continent, which is far from the ocean. The region has extremely low precipitation and a dry environment because of the impediment to moist air caused by plateaus and mountains and the effect of latitudinal-zone sinking air, forming huge deserts like the Gobi Desert. Consequently, such arid and semi-arid regions frequently experience dry and dusty weather, which has turned them into the main sources of aerosols [19–21].

High concentrations of aerosols have a negative impact on human health and life, and it has been proved that they cause more people to contract respiratory diseases [22–24]. In recent years, the number of aerosols increased significantly in China because of the rapidly growing economy, population, energy consumption, and exhaust emissions [25]. In China, the distribution of aerosols exhibits significant spatial and temporal variabilities [26,27]. Therefore, it is crucial to analyze the spatial–temporal distribution of aerosols and their influencing factors and to come up with appropriate solutions in order to regulate aerosol emissions effectively.

AOD indicates the atmospheric columnar aerosol load from the surface to the top of the atmosphere, which can be measured via remote sensing techniques, e.g., the LANDSEA comparison method [28], the structure function method [29,30], the dual multichannel reflectance method [29–33], and the dark target method (DT algorithm) [34,35]. Kaufman and Sendra [34] proposed an algorithm to automatically correct atmospheric errors in satellite images after continuous development and improvement. Pozzer et al. [36] studied the trend of global and regional AOD from 2001 to 2010 using an atmospheric model. Chubarova et al. [37] verified the accuracy of satellite-based aerosol extraction over Moscow, Russia, using observed aerosol data collected from the AERONET Aerosol Observation Station. Li et al. [38] examined the seasonal patterns of AOD using data from the Moderate-Resolution Imaging Spectroradiometer (MODIS). Zhang et al. [39] discovered the interactive relationship of AOD with clouds and precipitation. Bai et al. [40] employed spaceborne lidar data from Cloud-Aerosol Lidar Infrared Pathfinder Satellite Observations (CALIPSO) to characterize AOD in the arid areas of Northwest China. Most of the AOD studies in China have focused on Eastern China because of its large population, greater development, and higher anthropogenic emissions [41–43]. Zhang et al. [39] noted that aerosol concentrations in Western China are primarily caused by natural factors such as dust aerosols. However, most of these studies, especially those conducted in arid and semi-arid regions, did not further investigate the factors affecting AOD changes.

Li et al. [44] found that the MODIS Collection 5 (C005) product outperformed the MODIS C004 product in AOD estimation. Conversely, MODIS Collection 6 (C006) is superior to MODIS C051 [45]. Therefore, this study aims to evaluate the spatial–temporal changes in AOD over the arid region of Northwest China (ARNC) from 2008 to 2017 using MODIS C006 dual fusion algorithm products. Additionally, the majority of AOD factor analysis research conducted in China has considered only a single factor, either artificial or natural [21,42]. In order to provide a thorough AOD factor analysis, this study took into account both natural (precipitation, air temperature, relative humidity, wind speed, topography, NDVI, LST) and human (gross domestic product, population, proportion of secondary industry) factors. The findings could serve as a guide for the local authorities in formulating policies to reduce air pollution in ARNC.

2. Study Area

The ARNC, located in the ranges 35–50° N and 73–107° E, is a very important part of the arid central region of the Asian continent (Figure 1). The total area of arid land in Northwest China is about 2.5×10^6 km², accounting for approximately 25% of China's land area [46], as shown in Figure 1. It is located north of the Qilian Mountains and Kunlun–Altun Mountains and west of the Helan Mountains. The ARNC includes the entire Xinjiang Uygur Autonomous Region (hereinafter referred to as Xinjiang), the five cities of Gansu Hexi, and the huge Alashan League in Inner Mongolia [47]. The ARNC is limited by the border of China to the north and west. The northwest arid area is an inland area with less than 400 mm/year of annual precipitation [48], belonging to the extremely arid area. From east to west, the land-use types include grassland, desert steppe, desert, Hulunbeir Grassland, rocky Gobi, sand dune, inland river, inland lake, and oasis. The natural vegetation is gradually decreasing because of human activity.

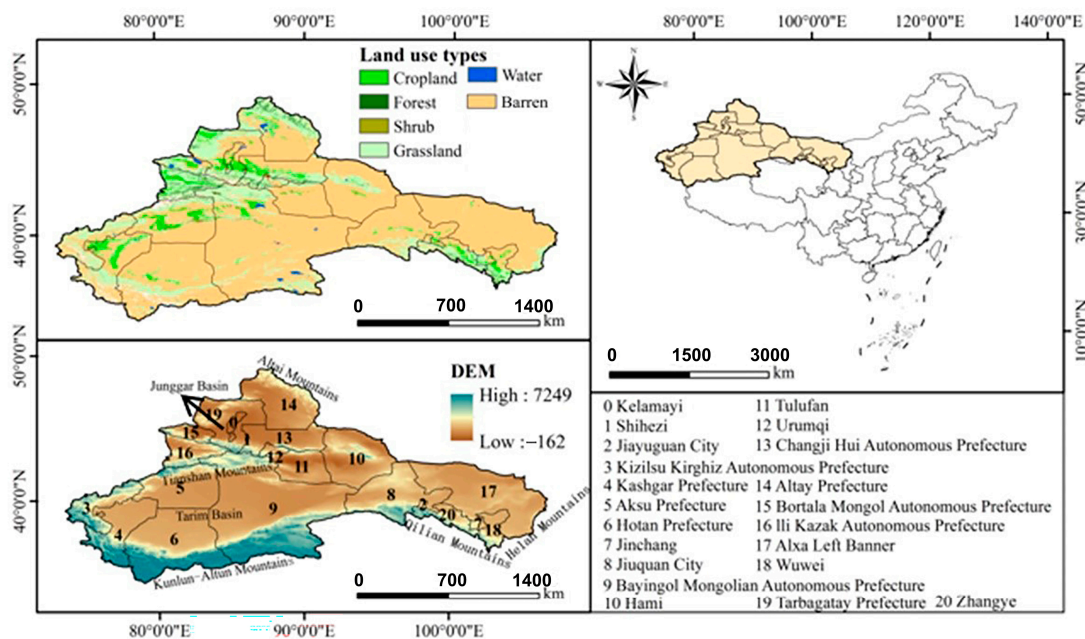


Figure 1. Sketch map of the study area.

3. Data Sources and Methods

3.1. Remote Sensing Data

MODIS C006 products from 2008 to 2017 were downloaded to extract the “AOD_550_Dark_Target_Deep_Blue_Combined_Mean_Mean” band. MODIS C006 is a dual fusion product based on NDVI (normalized difference vegetation index) data, combining the DT and DB algorithms. The data product is atmospherically corrected and has some reliability and scientific validity [49]. The MODIS C006 products’ data source is the Level-1 and Atmosphere Archive & Distribution System Distributed Active Archive Center (<https://ladsweb.modaps.eosdis.nasa.gov/>, accessed on 1 October 2023). The spatial resolution of the monthly mean AOD raster image data at 550 nm is 1° × 1° [49]. The data quality is good in the mid-latitude region, with minimal missing values. In addition, Tao et al. [50] found that this data band is suitable for large-scale aerosol studies in bright surface deserts and urban areas.

The relationship between topography and AOD was examined using the Shuttle Radar Topography Mission (SRTM) 250 m resolution digital elevation model (DEM) provided by the Consultative Group on International Agricultural Research (CGIAR). The SRTM DEM is widely used in the surveying and mapping disciplines [51]. A total of 120 MODIS NDVI MYD13C2 composite images (0.05° × 0.05°) covering the entire study area were obtained from NASA every 8 days from 2008 to 2017. Monthly LST (land surface temperature) data were extracted from the fifth version of MODIS’s daytime surface temperature data from the MODIS Aqua satellites. The accuracy of the product was verified, confirming that it is suitable for research in the ARNC [52].

3.2. Auxiliary Data

Daily meteorological data such as precipitation, relative humidity, air temperature, and wind speed from 2008 to 2017 were collected from the China Meteorological Data Network (<http://data.cma.cn/>, accessed on 19 October 2023). Socioeconomic data included population density data and local GDP (Gross Domestic Product) data. The proportion of manufacturing industry in the GDP of each city in the northwest arid area was extracted from the statistical yearbooks of cities. The specific sources of the above data are shown in Table 1.

Table 1. Data products used in this study.

Data Product Types	Scientific Data Set (SDS)	Attribute	Data Acquisition	Use
MYD08_M3	AOD_550_Dark_Target_Deep_Blue_Combined_Mean_Mean https://ladsweb.modaps.eosdis.nasa.gov/search/order/1/MYD08_M3--61	Monthly time resolution 1° spatial resolution	2008.1–2017.12	Calibration of spatio-temporal characteristics and influencing factor analysis.
SRTM data	https://ladsweb.modaps.eosdis.nasa.gov/search/order/	Annual time resolution 250 m spatial resolution	2020	Analysis of the influence of the DEM on AOD.
MYD13C2	CMG 0.05 Deg Monthly NDVI std dev https://ladsweb.modaps.eosdis.nasa.gov/search/order/1/MYD13C2--6	8-day time resolution 0.05° spatial resolution	2008.1–2017.12	Analysis of the influence of NDVI on AOD.
MYD11C3	Cloud-Top_Temperature_Nadir_Day_Mean_Mean https://ladsweb.modaps.eosdis.nasa.gov/search/order/1/MYD11C3--0	Monthly time resolution 0.05° spatial resolution	2008.1–2017.12	Analysis of the influence of land surface temperature on AOD.
Daily dataset for China surface climatic data released by the China Meteorological Data Network	Precipitation, Relative humidity, Temperature, Wind speed http://data.cma.cn/	Daily time resolution	2008.1.1–2017.12.31	Analysis of the influence of meteorological factors on AOD.
China Statistical Yearbook	The proportion of secondary industry, GDP, Population Density https://www.cnki.net/	Annual time resolution	2009–2018	Analysis of the influence of socioeconomic factors on AOD.
Topographic and geomorphological data	Resource and Environment Science and Data Center https://www.resdc.cn/	Annual time resolution	2009–2018	Analysis of the correlation between meteorological factors and AOD in different territories.

3.3. Methods

3.3.1. Mean Value Method

Based on monthly scale raster data, the mean value method was used to obtain the annual and quarterly spatial distribution of AOD in the ARNC from 2008 to 2017. In addition, data on the influencing factors were also obtained using the same method. The mean value method can make the analysis process simpler, which was achieved through tools in the ArcGIS 10.8 software [53]. The principle is to use multi-year data combined to obtain the average value instead of multi-year AOD, NDVI, LST, etc.

3.3.2. Trend Analysis and Significance Test

The linear trend estimation method has excellent applicability in the study of spatial-temporal changes in AOD, and the method has a large research base [42,54–56]. Therefore, one-dimensional linear regression analysis was used to analyze the trends in AOD with two scales: the region as a whole and the raster cells. The calculation formula is shown below [57]:

$$\theta_{slope} = \frac{nx_i \sum_{i=1}^n i - \sum_{i=1}^n x_i \sum_{i=1}^n i}{n \sum_{i=1}^n i^2 - (\sum_{i=1}^n i)^2} \quad (1)$$

where θ_{slope} is the trend value. When $\theta_{slope} > 0$, AOD shows an increasing trend. When $\theta_{slope} = 0$, AOD shows no change. When $\theta_{slope} < 0$, AOD shows a decreasing trend. x_i denotes the AOD value in year i , and n is the total number of years ($n = 10$ in this paper). According to the slope evaluation results, combined with the significance test, the slope can be divided into five grades (see Table 2 for details).

Table 2. Linear trend estimation process.

Level	Description
$\theta_{slope} < 0, p < 0.01$	Significant decrease
$\theta_{slope} < 0, 0.01 \leq p < 0.05$	Slight decrease
$0.05 \leq p$	Basically unchanged
$\theta_{slope} > 0, 0.01 \leq p < 0.05$	Slight increase
$\theta_{slope} > 0, p < 0.01$	Significant increase

Note: p indicates the level of the significance test.

3.3.3. Correlation Analysis

In this paper, the correlation coefficients (R) of AOD and its influencing factors were calculated with multiple scales. On the one hand, they were calculated based on two time scales: annual and seasonal. On the other hand, they were calculated based on two time scales: regional overall and image element. Thus, the interrelationship between AOD and its influencing factors can be measured. The calculation formula [43,58,59] is

$$R = \frac{\sum_{i=1}^N [(X_i - \bar{X})(Y_i - \bar{Y})]}{\sqrt{\sum_{i=1}^N (X_i - \bar{X})^2 \sum_{i=1}^N (Y_i - \bar{Y})^2}} \tag{2}$$

where X, Y, \bar{X} , and \bar{Y} denote two variables and the mean of the variables, respectively; R is the correlation coefficient between the variables X and Y ; and N is the sample size. The correlation is considered significant when $p < 0.05$.

The framework of this study is visualized in Figure 2. The study was conducted in four major steps: (1) reconstruction of annual and seasonal average AOD grid maps with ArcGIS tools; (2) analysis of the slope of the AOD changes at the regional and pixel scales to reveal spatial-temporal variation; (3) resampling of the DEM, NDVI, and LST data to a spatial resolution of $1^\circ \times 1^\circ$ [60]; and (4) an evaluation of the correlation between AOD and its influencing factors using the correlation coefficient (R) approach. The R values vary from 0 to 1, with 1 representing a perfect correlation between AOD and its driving factors.

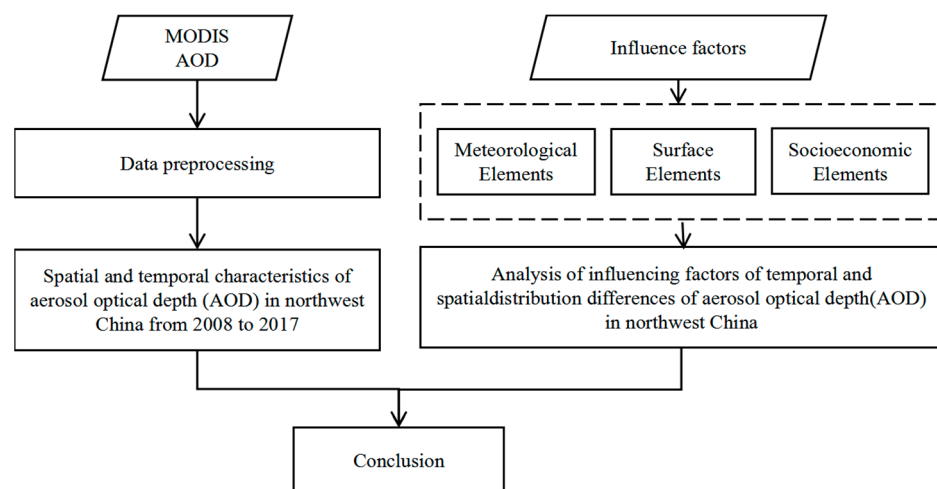


Figure 2. The framework of the study.

4. Results and Analysis

4.1. Spatial Distribution Characteristics of AOD in the ARNC

A spatial distribution map of AOD in the ARNC from 2008 to 2017 is shown in Figure 3. MATLAB was used to calculate the pixel-by-pixel trend in AOD. The results show that the Taklimakan Desert region consistently had high AOD during the studied period (Figure 3), particularly during spring. The reason could be the excessive sand- and dust-gusting phenomena in spring, which increase atmospheric turbidity, leading to high AOD values. Likewise, in summer, the AOD values east of the Taklimakan Desert and the Karamay and Tacheng areas are higher than in the west. In autumn, the AOD values from the western edge of the Taklimakan Desert are higher than in other regions. However, in winter, the Bayingolin Mongolian Autonomous Prefecture area had the highest AOD values compared with other areas. The reason for the significant regional variance in AOD in the ARNC is closely related to the contribution of sand and dust from the Taklimakan Desert, the main source of aerosol in Northwest China.

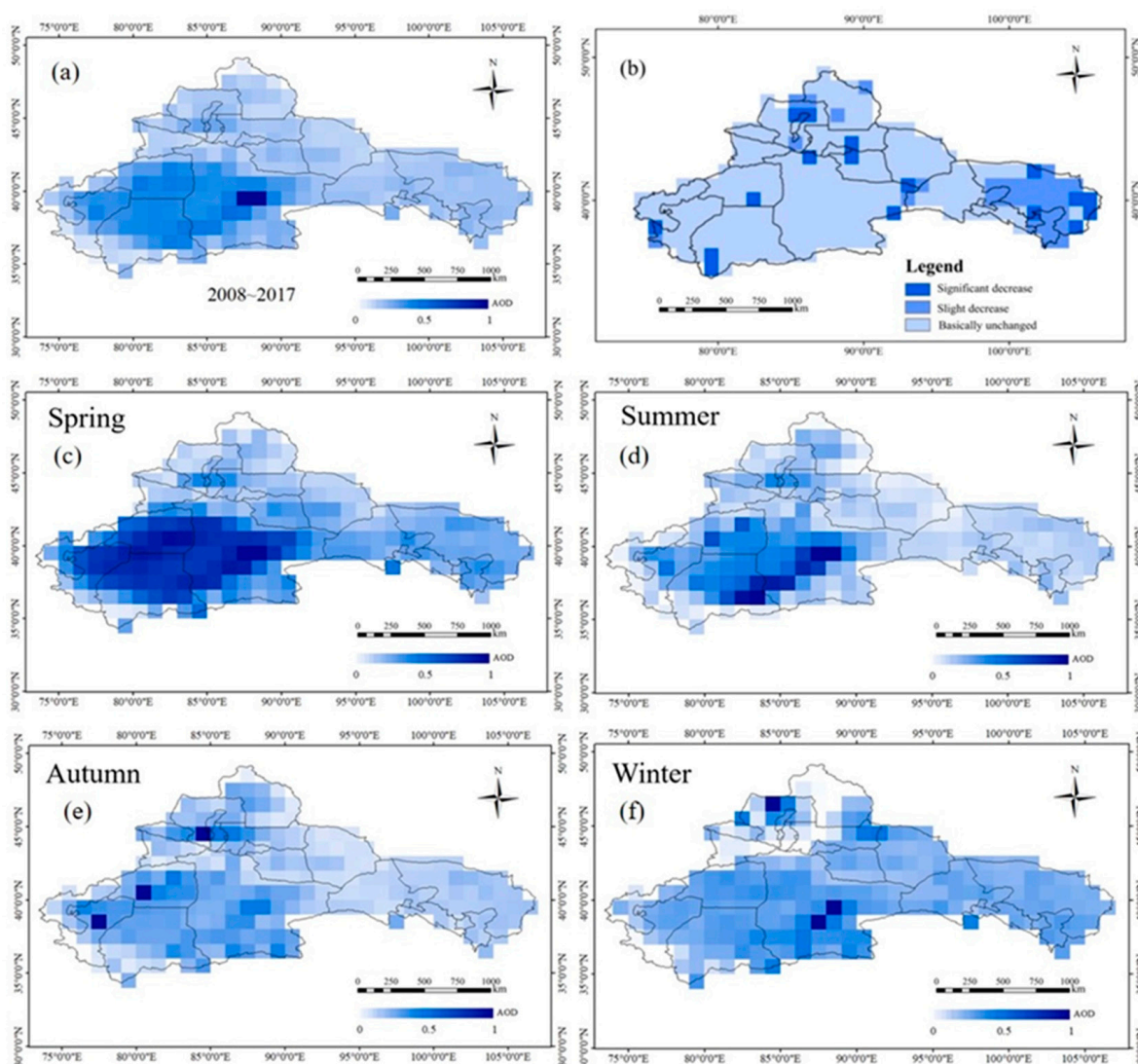


Figure 3. Variation trends in AOD in the ARNC from different years and different seasons ((a) spatial distribution of AOD during 2008–2017; (b) distribution of change trend types; (c–f) spatial distribution of AOD in different seasons).

Interestingly, from 2008 to 2017, a significant decrease trend in AOD values was observed along the northern part of the Tianshan Mountains and around the Gurbantunggut Desert in the Junggar Basin, while a slight decreasing trend in AOD values was observed in the Taklamakan Desert, located in the Tarim Basin. In contrast, in the eastern part of the study area, the AOD values in the area around Alxa Left Banner showed slight and significant decreases in a more concentrated manner. In other areas, the AOD values were unchanged. In general, the AOD values of ARNC showed a decreasing trend, particularly surrounding the desert region, proving the success of the mitigation treatment of the desert region in the past ten years.

To understand the spatial variation trend in AOD in ARNC, we further examined the statistics of AOD changes. Figure 4 shows that the areas with a significant decreasing trend from 2008 to 2017 in AOD accounted for 7.3% of the total area and 12.45% of the areas with a slight decreasing trend. The areas with no significant changes accounted for 80.26% of the total area. The AOD values in the Gobi Desert areas of the ARNC were basically unchanged, but in the desert edge areas, the aerosol content was effectively controlled through ecological restoration projects such as wind prevention and sand fixation.

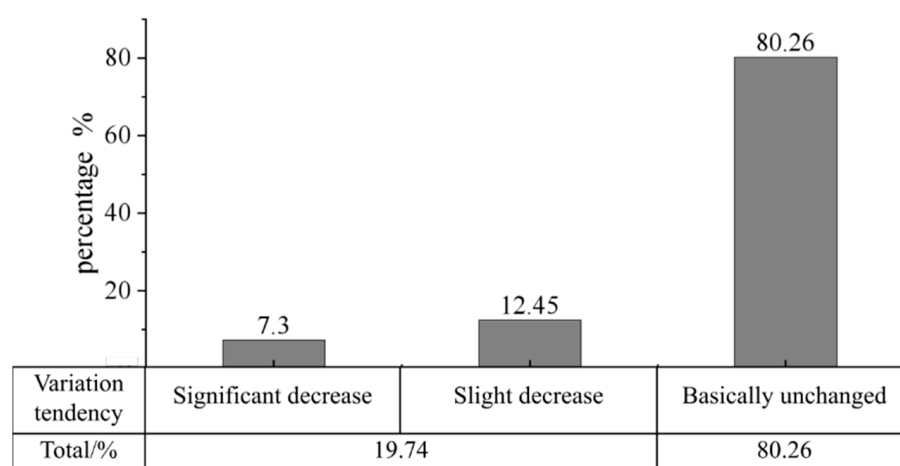


Figure 4. Areas of variation trends in AOD values in the ARNC during 2008–2017.

4.2. Temporal Variation in AOD in the ARNC

Table 3 shows the annual and seasonal average AOD of the ARNC from 2008 to 2017. The results show that the highest annual average AOD values in the northwest arid region were found in 2010, whereas the lowest were found in 2017. Seasonally, spring had the highest AOD values in the northwest arid region, followed by summer, while autumn and winter had the lowest values. The highest AOD value was found in spring 2014, with an average value of 0.46. In the summer, the highest AOD value was recorded in 2014, and the lowest value was in 2017. In autumn, the AOD value was highest in 2013 and the lowest value in 2015. The winters of 2010 and 2014 experienced the highest and lowest AOD values, respectively. The standard deviation of AOD in spring and summer is larger than in autumn and winter, indicating that the AOD changes in spring and summer are more significant than in autumn and winter. As can be seen from Table 3, although AOD fluctuated from 2008 to 2017, the overall changing trend was not large, with a certain decreasing trend. Discarding the impact of the external environment, this shows that the air quality improved slightly in the past ten years in the ARNC because of achievements in ecological civilization construction [61].

Table 3. Mean \pm standard deviation of AOD values annually and seasonally in the ARNC.

Years	Spring	Summer	Autumn	Winter	Annual
2008	0.44 \pm 0.25	0.24 \pm 0.16	0.13 \pm 0.06	0.16 \pm 0.10	0.24 \pm 0.12
2009	0.41 \pm 0.21	0.25 \pm 0.15	0.15 \pm 0.06	0.14 \pm 0.08	0.24 \pm 0.11
2010	0.45 \pm 0.29	0.27 \pm 0.20	0.17 \pm 0.11	0.17 \pm 0.12	0.26 \pm 0.16
2011	0.46 \pm 0.29	0.27 \pm 0.19	0.14 \pm 0.06	0.17 \pm 0.11	0.26 \pm 0.14
2012	0.45 \pm 0.30	0.22 \pm 0.14	0.16 \pm 0.07	0.14 \pm 0.09	0.24 \pm 0.13
2013	0.42 \pm 0.26	0.21 \pm 0.12	0.19 \pm 0.10	0.14 \pm 0.08	0.24 \pm 0.12
2014	0.46 \pm 0.23	0.28 \pm 0.18	0.17 \pm 0.08	0.13 \pm 0.08	0.26 \pm 0.13
2015	0.38 \pm 0.23	0.25 \pm 0.18	0.13 \pm 0.06	0.13 \pm 0.09	0.22 \pm 0.13
2016	0.42 \pm 0.30	0.23 \pm 0.14	0.13 \pm 0.06	0.17 \pm 0.11	0.24 \pm 0.13
2017	0.29 \pm 0.19	0.19 \pm 0.12	0.13 \pm 0.06	0.13 \pm 0.08	0.19 \pm 0.09
Mean (2008–2017)	0.42 \pm 0.24	0.24 \pm 0.15	0.15 \pm 0.06	0.15 \pm 0.08	0.24 \pm 0.12

4.3. Analysis of the Influencing Factors of AOD

4.3.1. Impact of Meteorological Factors on AOD

Figure 5 shows the temporal changes in meteorological variables from 2008 to 2017 in the ARNC. The annual average temperature was around 8 °C in 2011, which was the lowest in the studied period. Both 2008 and 2012 recorded low average annual temperatures as well, whereas the two warmest years on record were 2015 and 2016, followed by around 8.8 °C. The maximum annual precipitation corresponds to the maximum annual relative humidity that occurred in 2010 and 2016, with precipitation close to 165 mm/year and a relative humidity of about 50%. Less precipitation and low relative humidity (46%) were seen in 2009 and 2014. In 2013, the northwest arid region experienced low wind speeds, ranging from 2.1 m/s to 2.2 m/s. Meanwhile, the wind speed in 2017 was 2.48 m/s, which was the highest in the past decade.

From 2008 to 2017, all meteorological variables showed an increasing trend. Meteorological factors showed a certain regularity at an annual scale with different degrees. The changes in seasonal AOD all show decreasing trends. Overall, it was shown that the inter-annual variation in AOD decreased from 2008 to 2017, with a decreasing trend becoming obvious since 2013.

Figure 6 indicates that the meteorological variables have a relatively close relationship with AOD in spring, where air temperature, wind speed, relative humidity, and precipitation are all negatively correlated with AOD. In summer, air temperature and wind speed are positively correlated with AOD, indicating that AOD increases as air temperature and wind speed increase. In autumn, precipitation and wind speed are negatively correlated with AOD, and air temperature is positively correlated with AOD. The correlation between relative humidity and AOD is not obvious in summer. All the meteorological factors are positively correlated with AOD in winter, except air temperature.

The annual average AOD is positively correlated with both air temperature and wind speed, with the correlation coefficients being 0.33 and 0.80, respectively. The correlation coefficient between the annual average AOD and relative humidity is -0.77 , showing that the two variables are strongly negatively associated. On the inter-annual scale, the correlation between AOD and precipitation is not obvious, but on the seasonal scale, precipitation is closely related to AOD. There is, therefore, no consistent correlation between AOD and meteorological factors. Thus, different meteorological factors have distinct impacts on AOD [62].

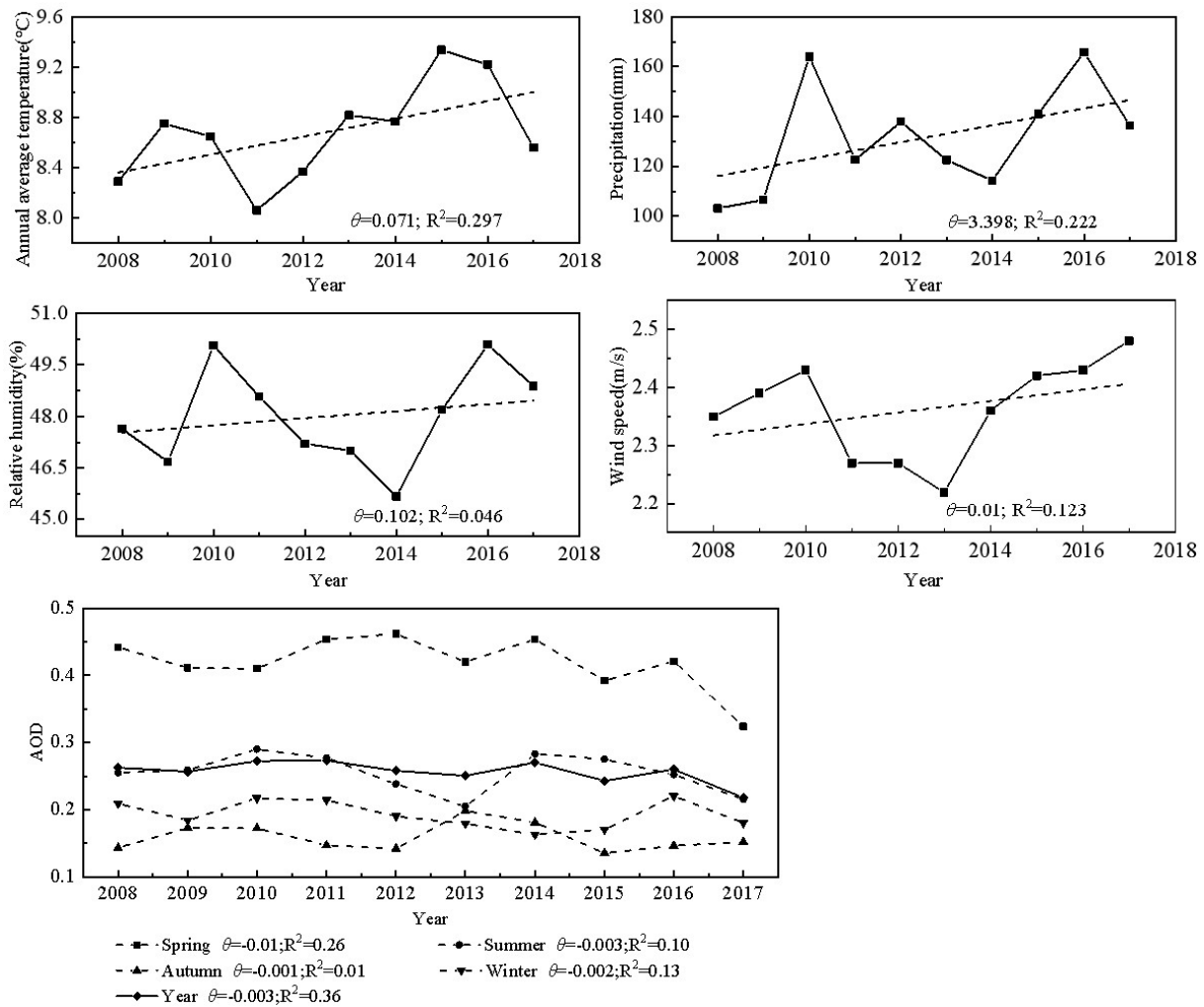


Figure 5. Meteorological elements and their seasonal AOD change trends in the northwest arid region from 2008 to 2017.

Considering the differences in meteorological elements across the ARNC, we extracted meteorological stations using topographic and geomorphological data and discussed the correlation between AOD and meteorological elements in highlands, plains, and deserts. In addition, the correlation between AOD and the statistical indicators was also further discussed for Northern Xinjiang, Southern Xinjiang, Gansu, and Inner Mongolia, because of variations in development levels in the ARNC.

As shown in Figure 7, AOD and precipitation showed a negative correlation in different subzones, AOD and temperature showed a positive correlation in the three regions, and AOD and wind speed showed a positive correlation in separate territories. To some extent, this demonstrates the inconsistent effects of meteorological factors on AOD and the different mechanisms of AOD generation in different subdivisions [63].

In Figure 8, both Northern Xinjiang and Southern Xinjiang show a positive correlation between AOD and GDP and between AOD and population, but Gansu and Inner Mongolia show a negative correlation. The reason why AOD and GDP and AOD and population do not show consistent and defined performance in different districts is that aerosol sources in the ARNC are dominated by natural sources [64].

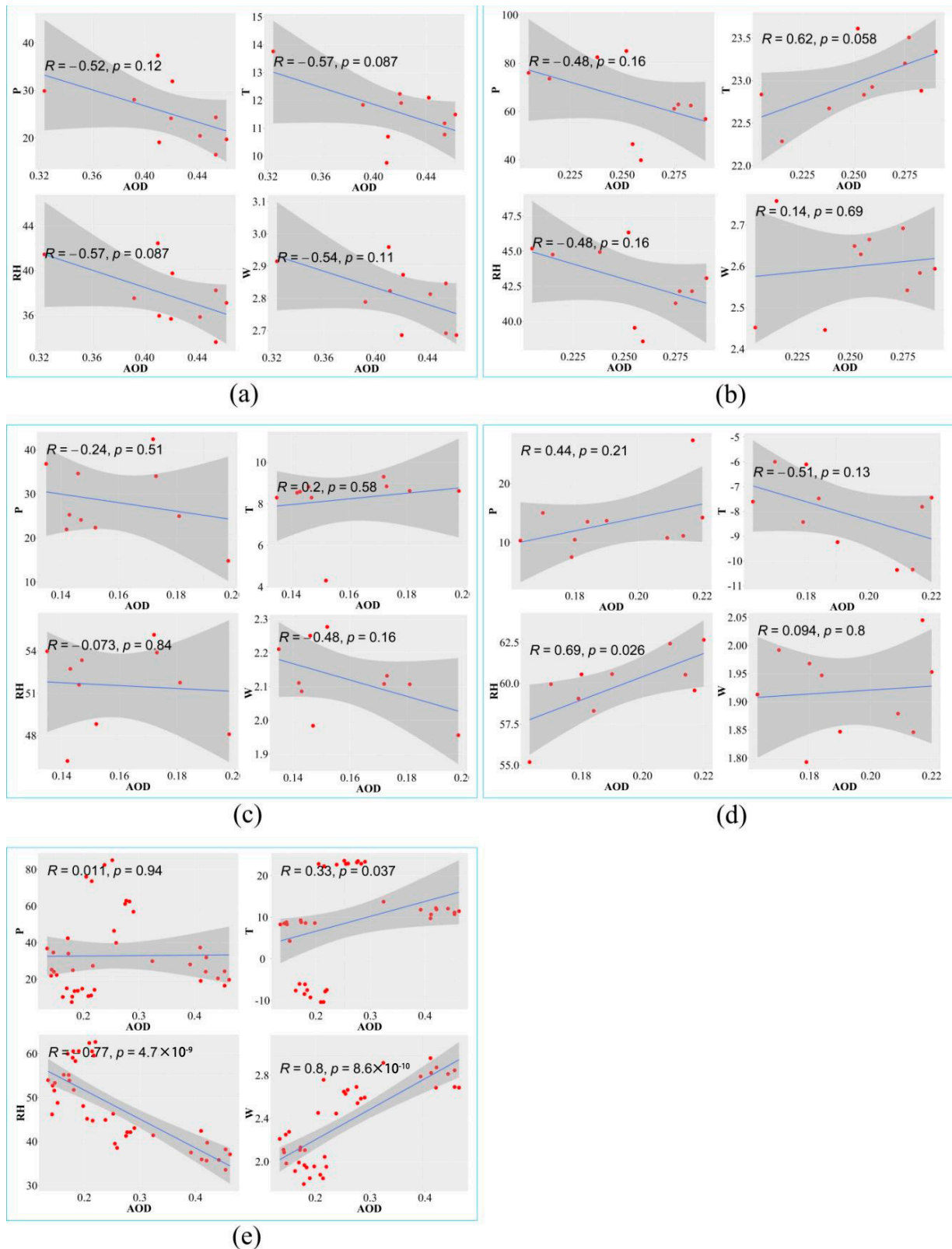


Figure 6. Correlation between AOD and meteorological factors. (a) spring; (b) summer; (c) autumn; (d) winter; (e) annual. Note: P, precipitation (mm); T, temperature (°C); RH, relative humidity (%); W, wind speed (m/s). Note: The red dots indicate the specific values for each data point, the gray bands indicate the confidence intervals for the linear regression, and the line indicates the regression line obtained by fitting a linear regression.

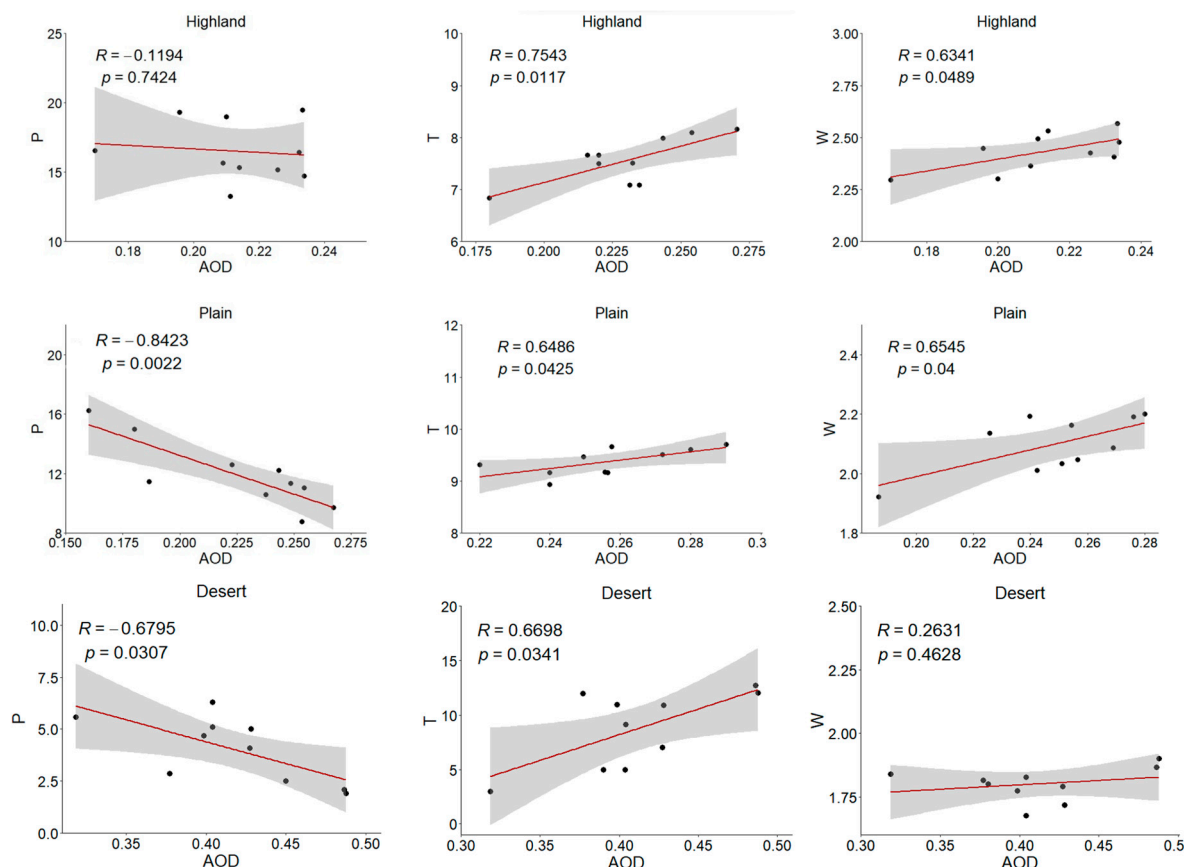


Figure 7. Correlations between AOD and meteorological factors in highlands, plains, and deserts in the ARNC. Note: P, precipitation (mm); T, temperature ($^{\circ}$ C); W, wind speed (m/s). Note: The black dots indicate the specific values for each data point, the gray bands indicate the confidence intervals for the linear regression, and the line indicates the regression line obtained by fitting a linear regression.

The seasonal trends in AOD and various meteorological factors are shown in Figure 9. As mentioned earlier, rainfall is low and scarce in the ARNC [65], so the impact of precipitation on AOD is small. Precipitation has a wet sedimentation effect on aerosols, so suspended particles in the air will be reduced to a certain extent [66], which is negatively related to AOD. Although the amount of precipitation is almost the same in spring and autumn, AOD is much higher in spring because of strong winds and low relative humidity. In summer, both precipitation and temperatures are high, so the relative humidity of the air and the AOD value are closely correlated. This may be because high temperatures promote evaporation, while suspended particles quicken the formation of precipitation, leading to a situation where water vapor in the air interacts with suspended particles in order to form aerosols. This indicates that there is a synergistic or inhibitory effect among various factors, which can affect AOD changes through indirect effects on other factors [67].

The correlation between wind speed, relative humidity, and AOD was found to be particularly strong. Strong winds will increase dust particles in the air and increase AOD, but an increase in relative humidity in the air will lead to a decrease in the dust wind speed [68]. The gathering interval of extremely high wind speeds shows a decreasing trend, while the relative humidity of the air has an increasing trend. It was found that AOD and wind speed are positively correlated with seasonal changes, whereas AOD is negatively correlated with relative humidity. Thus, there is a certain relationship between them. When the relative humidity in the air is high, the effect of wind in raising dust will be weakened, which produces a decreasing AOD trend with seasonal changes.

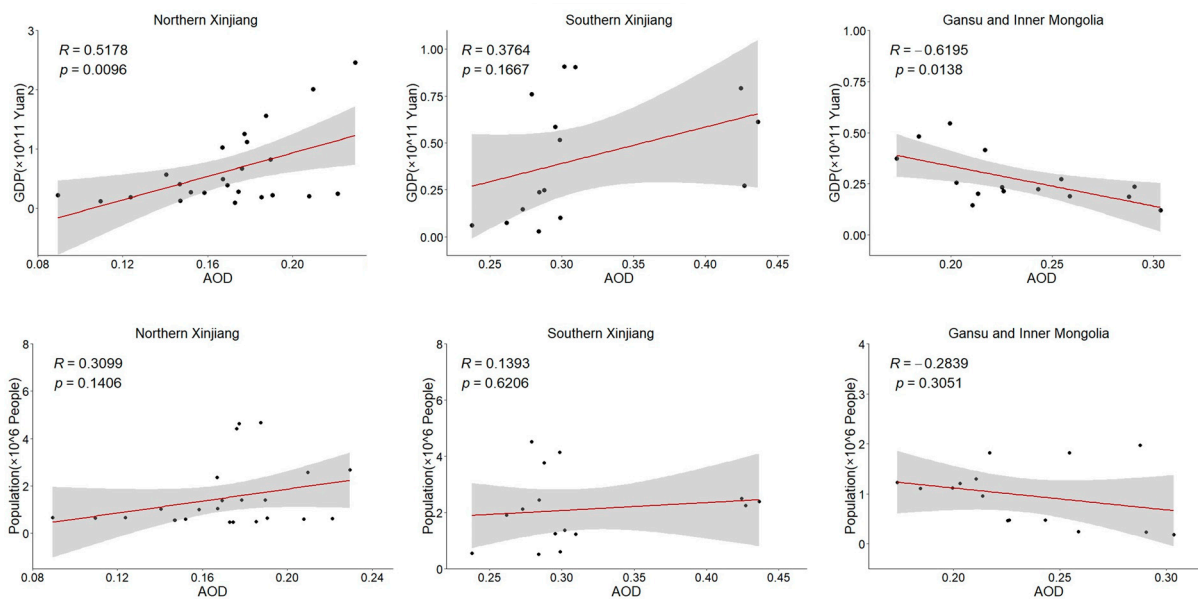


Figure 8. The links between inter-annual variations in AOD and GDP and AOD and total population separated by different parts of the ARNC. Note: The black dots indicate the specific values for each data point, the gray bands indicate the confidence intervals for the linear regression, and the line indicates the regression line obtained by fitting a linear regression.

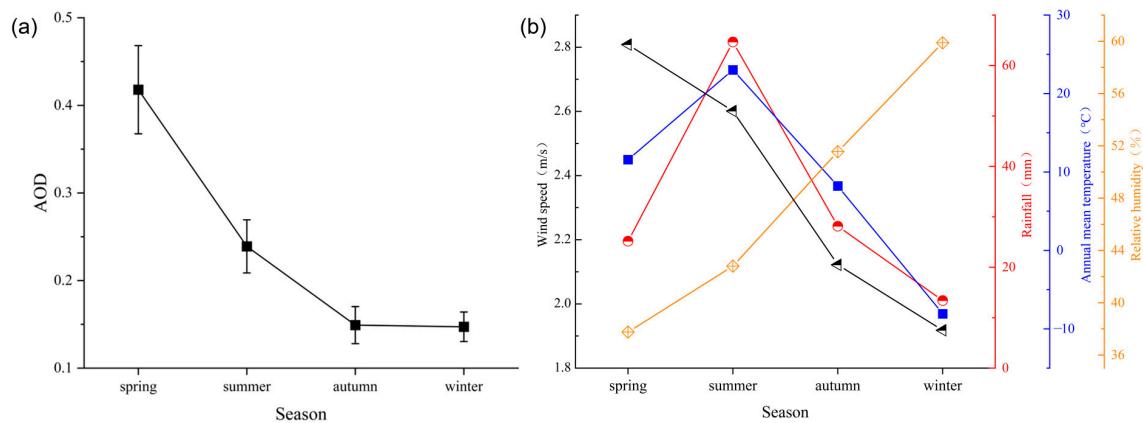


Figure 9. Seasonal variation in AOD (a) and meteorological factors (b). The color of the line corresponds to the color of the axes and indicates the change in the axis variable.

AOD is positively correlated with temperature, where the higher the temperature, the greater the AOD. Temperature affects the chemical properties of the gas in the air, changes the transfer of various particles in the air, and thus changes the AOD. When the temperature is high, the precipitation is likely to change at the same time. The high-temperature and high-humidity environment will make the aerosols gather to a certain extent [69]. A higher temperature has a critical impact on dust lifting [65], and dust is also susceptible to the influence of wind. An increase in the concentration of various particles in the air enhances the AOD value.

4.3.2. Influence of Surface Factors on AOD

The distribution of AOD shows obvious spatial differences in the ARNC, which is closely related to the underlying surface. LST, terrain fluctuations, and vegetation coverage all have an impact on the formation and development of aerosols. The findings show that AOD is positively correlated with surface elevation and surface temperature and negatively correlated with the NDVI. Figure 10a,d show that the distribution of AOD and topography

have clear similarities. High AOD values are mainly concentrated in the high-altitude areas, with significantly higher AOD values over the Altun Mountains, the Qilian Mountains, and the Kunlun Mountains. In contrast, AOD values are significantly lower in low-altitude areas such as the Altay and Hami areas. Figure 10b illustrates that DEM and AOD have a certain positive correlation, where the higher the region, the greater the AOD value. The reason for the high AOD values in high-altitude areas could be due to the influence of terrain, where the transported sand dust and other pollutants are prevented from spreading to other areas, thereby accumulating around the mountain areas [55].

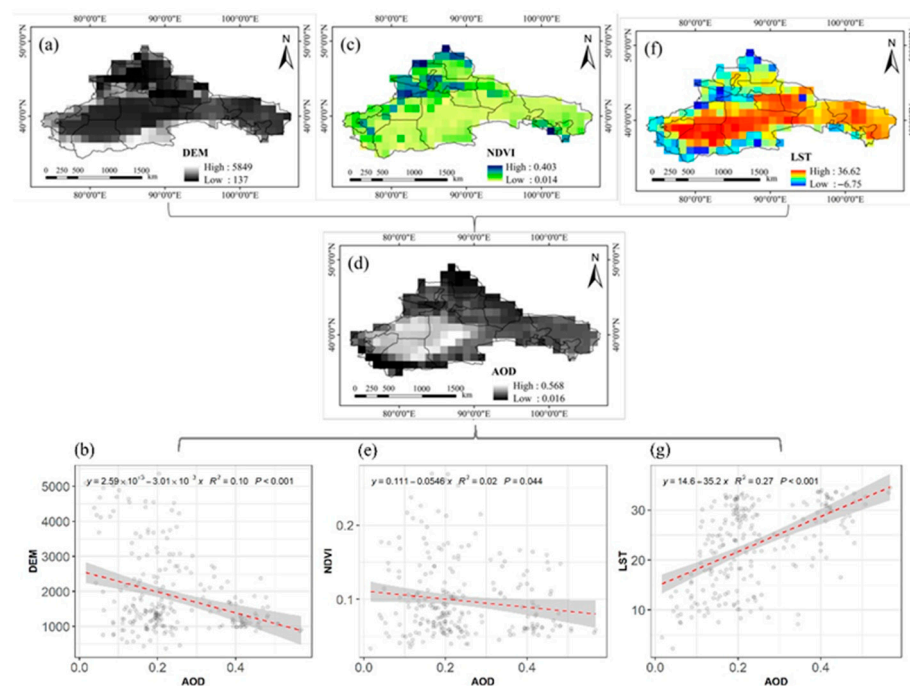


Figure 10. Correlation analysis of AOD and surface elements in the ARNC from 2008 to 2017. Note: (a), (c), (d) and (f) represent the spatial distribution of multi-annual mean values of DEM, NDVI, AOD and LST from 2007 to 2018, respectively. (b,e,g) are the results of correlation analysis of corresponding indicators.

MODIS NDVI images are used to reflect the vegetation situation in the ARNC. Figure 10c shows that the Ili, Northern Tianshan, Altay, and Weiku Oasis regions have relatively more vegetation and forests, especially the eastern region of Ili. Additionally, it can be seen that the Tarim Basin has high AOD values in all seasons because of the basin topography and sparse vegetation, which is not conducive to aerosol diffusion. The NDVI value did not significantly change from 2008 to 2017 in the ARNC (Figure 10e). In the Ili area, the NDVI value decreased, but the AOD value increased. In the Tarim Basin edge, the NDVI value increased, whereas the AOD value decreased. This indicates that there is a negative correlation between AOD and NDVI. Vegetation can block the direction of the wind, reduce wind speed, and weaken the process of dust aerosol formation. It can also reduce surface transpiration and affect the formation of relative humidity and precipitation in the air. In addition, vegetation can absorb aerosol particles in the air and accelerate their sedimentation process, thus reducing AOD [27,70]. This shows that changes in the ecological environment have a certain impact on AOD changes [71].

Figure 10f shows the spatial distribution of LST in the ARNC from 2008 to 2017. Affected by latitude and topography, the spatial distribution of LST has a certain degree of similarity to the spatial distribution of AOD. High-LST areas can be found in the Tarim Basin, Turpan, and the surrounding areas of Alxa League. The main reason is that these areas have a large proportion of desert and Gobi terrain, barren land, low vegetation coverage, and more solar radiation energy absorption. Interestingly, Figure 10g shows that

the higher the LST, the larger the AOD values, but the relationship between the LST and AOD is not perfectly correlated. In many areas, although the LST is high, the AOD value is still very small. This could be due to the fact that there are fewer human activities in the northwest region, which proves that the impact of human factors on the environment is small. In some cases, AOD has a weakening effect on the LST increases [69], as the result shows a weak correlation. Although the relationship between LST and AOD is weak, it has a significant impact on the formation and development of AOD. Given frequent drought occurrences in the northwest region, an increase in the surface temperature will have an impact on the underlying surface, promote the turbulent diffusion of aerosol particles in the area, and increase the value of AOD [72]. When the LST is high, the relative humidity of the air decreases, which inhibits the deposition of aerosols. In the desert and its surrounding areas, the LST is very high and is prone to dry hot air convection [73]. The high temperature can easily destroy the physical and chemical properties of the rocks and minerals, promoting the formation and diffusion of particles, which is very conducive to the formation of aerosols.

4.3.3. Impact of Socioeconomic Data on AOD

Table 4 shows the GDP and secondary industry output value of the ARNC from 2008 to 2017, where the GDP of the ARNC is increasing yearly. In 2008, the output value of secondary industry was CNY 2.747×10^{11} , but in 2017, the corresponding value increased to CNY 5.171×10^{11} . From 2011 to 2016, the proportion of secondary industry to GDP showed a decreasing trend, dropping to the lowest value in 2016, which was related to changes in regional industrial structure. The decline of the proportion of secondary industry considerably reduced many industries with high pollution emissions, and this not only improved the atmospheric environment but also reduced the aerosol content in the ARNC in recent years.

Table 4. Socioeconomic statistics data for the ARNC from 2008 to 2017 (unit: CNY 10^8).

Year	Gross Domestic Product	Secondary Industry Output Value	The Proportion of Secondary Industry to GDP	Per Capita GDP/CNY
2008	5319.88	2747.26	51.64%	9251.36
2009	5563.37	2705.26	48.63%	9109.94
2010	6944.07	3531.96	50.86%	11,893.84
2011	8449.14	4401.61	52.10%	14,822.38
2012	9631.03	4842.14	50.28%	16,305.88
2013	10,662.84	4932.91	46.26%	16,611.53
2014	11,520.33	5261.14	45.67%	17,716.84
2015	11,307.19	4539.85	40.15%	15,287.90
2016	11,655.08	4521.71	38.80%	15,226.83
2017	13,096.93	5171.40	39.49%	17,414.64

Figure 11 shows the regional AOD distribution and regional GDP, secondary industry, and population density statistics of the ARNC for 2008, 2012, and 2016. Here, the data are analyzed via equal-interval-selection-facilitated analysis. Figure 11a shows that the regional AOD decreased to a certain extent in 2016 compared with 2008. Urumqi had the highest GDP, and Ili Prefecture ranked second, but these two cities had higher AOD values. Furthermore, the GDP of the five cities in Hexi was also higher, corresponding to high AOD values as well, with AOD values above 0.2, whereas the GDP values of Turpan and Hami were low, so the effect of human economic activities in these areas is weak, with AOD values of 0.15. This demonstrates that there is a correlation between local GDP and AOD, with higher AOD in regions with higher GDP, which is mainly due to the production of heavy man-made aerosols produced by local economic activities (Figure 11b).

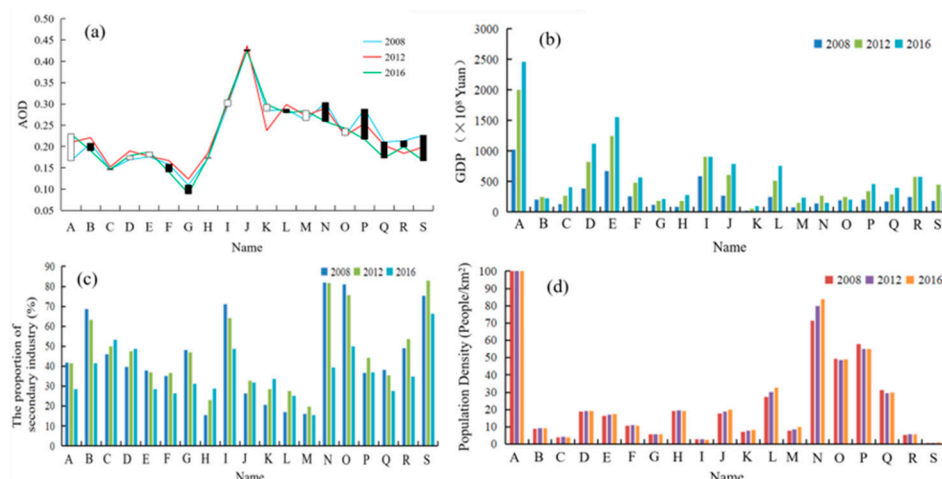


Figure 11. Statistics of AOD distribution, regional GDP, the gross product of secondary industry, and population density in the northwest arid region in 2008, 2012, and 2016. (a) AOD; (b) GDP; (c) the proportion of secondary industry; (d) population density. Note: A: Urumqi city; B: Turpan area; C: Hami area; D: Changji Prefecture; E: Yili Prefecture; F: Tachen area; G: Altay area; H: Bortala Mongol Autonomous Prefecture; I: Bayingol Mongolian Autonomous Prefecture; J: Aksu area; K: Kirgiz Prefecture; L: Kashi area; M: Hotan area; N: Jiayuguan City; O: Jinchang City; P: Wuwei City; Q: Zhangye City; R: Jiuquan City; S: Alxa League; same below.

Given the bar chart of the proportion of secondary industry in 2008, 2012, and 2016 (Figure 11c), it can be seen that the proportion of secondary industry in Turpan and Bayingol Mongolian Autonomous Prefecture was very high in 2008. In 2012, the proportion of secondary industry in Turpan and Bayingol Mongolian Autonomous Prefecture decreased slightly. By 2016, the proportion of secondary industry had decreased significantly. Given the changes in AOD in Turpan and Bayingol Mongolian Autonomous Prefecture, it is found that AOD in Turpan has declined, while AOD in Bayingol Mongolian Autonomous Prefecture has increased to a certain extent, but the range is still very small. This is related to the development of the local secondary industry, suggesting that the effect of industrial structure adjustment is very significant. The proportions of secondary industry were 41.7%, 41.4%, and 28.6% in Urumqi in 2008, 2012, and 2016, respectively, but given the influence of other human economic activities in Urumqi, the GDP increased rapidly, and its AOD values also increased. Among the five cities in the Hexi Corridor, Jiayuguan City and Jinchang City had a very high proportion of secondary industry in 2008 and 2012. After the adjustment of industrial structures, there was a significant decline in 2016. Compared with the AOD of 2008, AOD also decreased significantly, which shows that the development of secondary industry plays an important role in promoting the emergence and development of AOD. Secondary industry is the main body of resource consumption and environmental pollution. It is the largest energy consumption sector, and its pollution gases, such as sulfur dioxide and nitrogen oxides, are important factors in the increase in AOD. Thus, energy conservation, emission reduction, and the adjustment of industrial structure are important measures to reduce AOD.

Urumqi has the highest population density in the area, as shown in Figure 11d. The population density of Kashgar is slightly higher than that of other prefectures. However, the population density of the five cities in the Hexi Corridor is in the order of Jiayuguan City, Wuwei City, Jinchang City, Zhangye City, and Jiuquan City. Except for Jiuquan City, the other four cities in the Hexi Corridor are higher than those in Xinjiang, except Urumqi. Interestingly, Alxa League has a large area, but its population is very sparse. Comparing the population density with AOD distribution, it is found that the higher the population density, the higher the AOD values, especially in Kashgar and Hexi’s five cities. Although the population density is not large in Bayingol Mongolian Autonomous Prefecture, Aksu Prefecture, and Kizilsu Kirghiz Autonomous Prefecture, the AOD values are still high in

this region, which is related to the influence of sand and dust in the Taklimakan Desert. This study shows that the population is distributed spatially in the ARNC in a highly uneven distribution, with a generally low population density but a very high population density in some regions. As economic development is mostly concentrated in regional areas, AOD is greatly affected by human factors.

Figure 12 shows the relationship between the average annual GDP and total population in the high-population ARNC region and AOD. It can be seen that the average annual GDP and total population in the high-population area in Northwest China have no obvious relationship with AOD. In other words, being in an economically developed and populous area does not mean that AOD is high, indicating that the main source of aerosol in Northwest China is not caused by pollutant emissions from economic development. This also shows that the aerosol in Northwest China is mainly from dust aerosol [74,75].

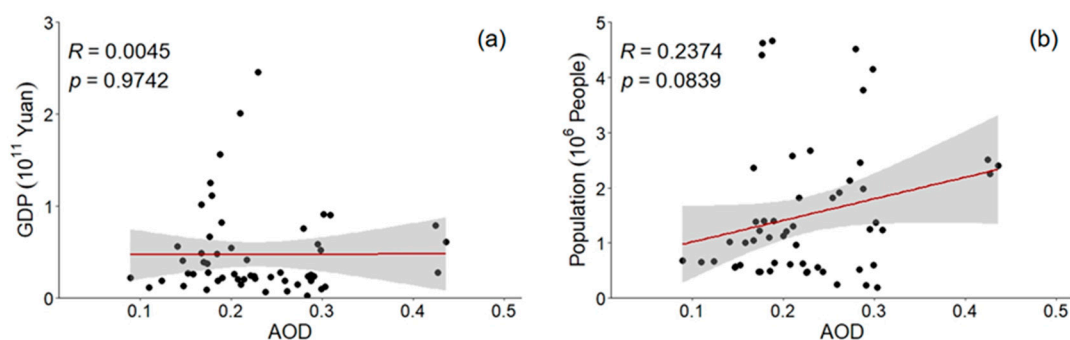


Figure 12. The links between inter-annual variations in AOD and GDP and AOD and total population averaged by highly populated parts of the ARNC (a) the correlation between AOD and GDOP; (b) the correlation between AOD and Population). Note: The black dots indicate the specific values for each data point, the gray bands indicate the confidence intervals for the linear regression, and the line indicates the regression line obtained by fitting a linear regression.

5. Discussion and Conclusions

5.1. Discussion

5.1.1. Spatial–Temporal Pattern Analysis

This study discovered the distinct spatial–temporal distributions of AOD in the ARNC. The seasonal variation in AOD is high in spring and low in summer, autumn, and winter. This is contrary to the findings reported by Zhang et al. [76], who found that AOD in winter is higher than in autumn, which may be related to the high data-loss rate of MODIS aerosol products in Northwest China. Although the method used in this study has some limitations, it is still of great value in large-scale research on the ARNC. In terms of spatial distribution, the AOD values of the Tarim Basin and its surrounding areas are the highest, showing a significant contribution to AOD in the whole northwest region. This is because the weather of the region is under the influence of frequent sand and dust storms, making the content of dust aerosol in the air high and resulting in high AOD values, which is consistent with the findings of Guo et al. [77].

When the spatial distribution of AOD is examined, it is found that elevation has a substantial impact on AOD. However, Zhang et al. [41] and Yue et al. [54] reported that the DEM has less impact on AOD in the central and coastal cities of China. The difference in terrain will affect regional climate and the temporal and spatial distribution of AOD. In addition, altitudinal differences also affect the range of human activities, and this, in turn, produces spatial distribution differences. Through correlation analysis, the DEM and AOD are found to be positively correlated. However, given the complex topography and large fluctuation of elevation in the ARNC, the average elevation of the lowest region is about 444 m, and the highest is more than 3000 m. The correlation coefficient is only 0.3948 between AOD and DEM data. This shows that the relationship is not that strong. In the quantitative analysis of AOD in areas with complex terrain and large drops, it is necessary

to consider the influence of the DEM. The difference in the vertical structure of AOD is obvious, and zoning analysis and discussion are needed in order to obtain better results.

5.1.2. Influencing Factor Analysis

In examining the influence of meteorological factors on AOD, it was found that wind speed and relative humidity have a good relationship with AOD on an annual scale, whereas the relationship between AOD and temperature and precipitation is weak on an annual scale but has a good correlation on a seasonal scale. Wind can affect the dust in the air and drive the increase in AOD, while relative humidity can affect wind speed. At the same time, this has an impact on precipitation via the promotion of the sedimentation of AOD, and this can reduce the AOD concentration. In spring and autumn, AOD in the region may not depend on emissions from the local deserts but instead relate to aerosol transport from remote areas during this period, considering that wind speed is negatively correlated with AOD. This mechanism shows that there is a synergistic or inhibitory relationship between various meteorological factors, which makes the driving analysis of aerosols more complicated [67]. For example, the correlation coefficient between precipitation and AOD on an annual scale is only 0.011, but on a seasonal scale, there is a close relationship between precipitation and AOD. Given the influence of other meteorological factors on precipitation in each season, the correlation between precipitation and AOD is weak on an annual scale, which is related to the complexity of climate types in Northwest China.

There is a close relationship between AOD and surface factors, such as changes in the surface environment. The DEM and LST are positively correlated with AOD. Around the mountains, AOD shows a trend of aggregation and has an obvious spatial distribution. Of the two, changes in LST can affect the distribution of particles in the underlying surface. The higher the LST, the easier it is for all kinds of particles to spread out, thus increasing AOD. There is a negative correlation between the NDVI and AOD, where the larger the ground vegetation coverage, the smaller the AOD value. This is because the regulating effect of vegetation on the environmental temperature and air humidity has a kind of purification effect on the environment and acts as a wind barrier [27]. Therefore, strengthening the protection of the ecological environment of the oasis area and increasing green areas will help to modify the micro-climate of the northwest region, leading to a reduction in the adverse effects of sand and dust weather and enhancing the ecological threshold of the northwest region.

Meteorological factors and surface environmental factors are closely related to AOD changes in the ARNC. For example, high wind speeds are related to mass concentrations of PM in the air. Either way, high-friction velocity for high-mass concentrations of natural dust vs. high ventilation effects lead to low mass concentrations. Since the surface variables are highly dependent on the meteorological variables, e.g., the NDVI is strongly correlated with precipitation, regression should be performed for AOD, surface variables, and meteorological variables together. Otherwise, it is hard to identify the root causes of AOD changes. To deal with this kind of problem, we can apply the existing model and consider the influence of wind speed, humidity, and the NDVI on dust particles in the air.

In recent years, the proportion of secondary industry in the GDP of Northwest China has decreased, and this has reduced AOD values in the region. The growth of the local population density and the development of GDP depends on the industrial development of the region, which can have an impact on AOD changes. Especially during winter in Northwest China, the combustion of large amounts of fuel and gas in areas with intense anthropogenic activities can lead to an increase in man-made aerosols in the air. The literature on aerosols research shows that the influence of human activities has a significant effect on aerosols [78]. The northwest region is vast, and cities are mainly concentrated in the oasis area. Although the impact of human activities is relatively small, it cannot be ignored. For example, in the inter-annual change in AOD, it was found that the overall trend in AOD decreased from 2008 to 2017, and the decreasing trend became obvious in 2013. This is related to the vigorous investment in environmental pollution control by provinces

and cities. According to the data of the China Statistical Yearbook, 2008–2017, after 2010, various regions vigorously rectified pollutant gas and industrial smoke emissions. As a result, air pollution was considerably reduced, reflecting the positive effect of effective environmental governance, which has also controlled the formation and development of aerosols in the air to a certain extent. This is evident in economically developed cities where the aggregation of AOD is more obvious. Achieving balance and coordination between the economy and the environment is a major problem in urban development.

5.1.3. Deficiency and Prospect

The AOD data are not compared with other independent observations, e.g., surface mass concentration, AERONET, other LEO satellite data, etc. Thus, it is impossible to evaluate the pixel-level quality, but the product data have been widely used and verified in previous studies [79]. According to the studies conducted by Feng and Zou [67] and Zhu et al. [80], other surface factors such as soil moisture can also affect aerosol concentrations in the air. In addition to affecting aerosol emission and deposition, surface factors can also indirectly affect aerosol by changing meteorological conditions, such as temperature and precipitation [62,81]. There are various land use types in Northwest China, but the effects of the soil layer and water content on AOD were excluded from this study. These parameters should be considered in the future for similar studies in Northwest China. Moreover, considering how much of the study area would be an unretrievable “bright surface” per the Dark Target algorithm, it might be worth trying the Deep Blue algorithm on its own, either in addition to or instead of the fusion product.

In future research, MODIS aerosol products can be used to plot the Ångström exponent, which is helpful in showing the differences between aerosol from desert dust and aerosol from combustion, and it might provide a clearer contrast between spring and winter. The correlation of AOD is also different in different elevation ranges, but the difference and correlation of AOD in the vertical structure need more experimental data and research, especially when studying the spatial–temporal variation characteristics of AOD in a larger range. Researchers should not only discuss the change factors in a horizontal structure but also analyze changes in a vertical structure. The quantitative analysis of AOD at different heights needs more follow-up research.

Natural factors follow a certain law of change in time variation, so the influence on AOD also shows a certain regularity in time variation. The impact of human factors on AOD can have sudden changes, and their effect on the natural environment also indirectly leads to changes in AOD. Thus, human factors do not necessarily show obvious effects in terms of time variation. In future research, the authors should identify and distinguish the interaction of various factors to better explore the physical mechanism of these driving forces, which are expected to provide a scientific basis for the management and control of aerosol pollution.

5.2. Conclusions

This study employed MODIS Aqua C006 aerosol product data from 2008 to 2017 and other meteorological, socioeconomic, and terrain data to analyze the factors influencing spatial–temporal changes in AOD in the ARNC. The specific conclusions derived from this study are as follows:

- (1) The AOD value in the Taklimakan Desert area remained high, but in the majority of ARNC regions, it basically remained unchanged, with a slight decreasing trend in the surrounding areas of the desert. AOD has obvious seasonal characteristics and is highest in spring, followed by summer, autumn, and winter.
- (2) In terms of the natural environment, AT, WP, LST, and DEM were significantly positively correlated with AOD, while precipitation, RH, and the NDVI were significantly negatively correlated with AOD. These results imply that, for different seasons, meteorological factors have different effects on AOD.

- (3) In terms of social economy, GDP, the output value of secondary industry, and PD are closely related to changes in AOD. This is especially true in areas with high population density, indicating that human factors have a more significant impact on AOD than other factors.

Overall, this study managed to show the temporal and spatial distribution of AOD and its influencing factors in the ARNC. The other results of this study showed the effects of various factors, which is helpful for decision-makers in formulating environmental policies to protect the air quality of Northwest China.

Funding: This research was carried out with financial support from the Strategic Priority Program of the CAS, the Pan-Third Pole Environment Study for a Green Silk Road (XDA20040400), and the Tianshan Talent Project (Phase III) of the Xinjiang Uygur Autonomous region.

Institutional Review Board Statement: Not applicable.

Informed Consent Statement: Not applicable.

Data Availability Statement: The data presented in this study are available on request from the corresponding author. The data are not publicly available due to the data sharing policy.

Acknowledgments: The author appreciates all anonymous reviewers for their helpful comments and suggestions. Meanwhile, the author would like to thank Xin He, Liyang Guo, and Jingchao Shi for providing helpful suggestions to improve this revised manuscript.

Conflicts of Interest: The author declares no conflict of interest in this work.

Abbreviation

AOD	Aerosol optical depth
DEM	Digital elevation model
ARNC	Arid region of Northwest China
AT	Air temperature
WP	Wind speed
LST	Land surface temperature
NDVI	Normalized difference vegetation index (NDVI)
GDP	Gross domestic product
PD	Population density
DT	Dark target
DB	Deep Blue
MODIS	Moderate Resolution Imaging Spectrometer
RH	Relative humidity
SRTM	Shuttle Radar Topography Mission
CALIPSO	Cloud-Aerosol Lidar Infrared Pathfinder Satellite Observations
CGIAR	Consultative Group on International Agricultural Research

References

1. Kaufman, Y.J.; Tanré, D.; Remer, L.A. Operational remote sensing of tropospheric aerosol over land from EOS moderate resolution imaging spectroradiometer. *J. Geophys. Res.-Atmos.* **1997**, *102*, 17051–17067. [[CrossRef](#)]
2. Streets, D.G.; Yan, F.; Chin, M. Anthropogenic and natural contributions to regional trends in aerosol optical depth, 1980–2006. *J. Geophys. Res. Atmos.* **2009**, *114*, 1159–1171. [[CrossRef](#)]
3. Shen, Y.; Zhang, L.P.; Fang, X. Long-Term Analysis of Aerosol Optical Depth over the Huaihai Economic Region (HER): Possible Causes and Implications. *Atmosphere* **2018**, *9*, 93. [[CrossRef](#)]
4. Omari, K.; Abuelgasim, A.; Alhebsi, K. Aerosol optical depth retrieval over the city of Abu Dhabi, United Arab Emirates (UAE) using Landsat-8 OLI images. *Atmos. Pollut. Res.* **2019**, *10*, 1075–1083. [[CrossRef](#)]
5. Grassl, H. Calculated circumsolar radiation as a function of aerosol type, field of view, wavelength, and optical depth. *Appl. Opt.* **1971**, *10*, 2542–2543. [[CrossRef](#)] [[PubMed](#)]
6. Pacyna, J.M.; Ottar, B. Origin of natural constituents in the Arctic aerosol. *Atmos. Environ.* **1989**, *23*, 809–815. [[CrossRef](#)]
7. Bond, T.C.; Streets, D.G.; Yarber, K.F.; Nelson, S.M.; Woo, J.-H.; Klimont, Z. A technology-based global inventory of black and organic carbon emissions from combustion. *J. Geophys. Res. Atmos.* **2004**, *109*, D14203. [[CrossRef](#)]

8. Schauer, J.J.; Rogge, W.F.; Hildemann, L.M.; Mazurek, M.A.; Cass, G.R.; Simoneit, B.R. Source apportionment of airborne particulate matter using organic compounds as tracers. *Atmos. Environ.* **2007**, *41*, 241–259. [[CrossRef](#)]
9. Lu, Z.; Streets, D.G.; Zhang, Q. Sulfur dioxide emissions in China and sulfur trends in East Asia since 2000. *Atmos. Chem. Phys. Discuss.* **2010**, *10*, 6311–6331. [[CrossRef](#)]
10. Lei, Y.; Zhang, Q.; He, K.B. Primary aerosol emission trends for China, 1990–2005. *Atmos. Chem. Phys.* **2011**, *11*, 931–954. [[CrossRef](#)]
11. Martin, W.; Barbara, T.; Atsumu, O. Global dimming and brightening: An update beyond 2000. *J. Geophys. Res. Atmos.* **2009**, *114*, 895–896. [[CrossRef](#)]
12. Kaiser, D.P.; Qian, Y. Decreasing trends in sunshine duration over China for 1954–1998: Indication of increased haze pollution? *Geophys. Res. Lett.* **2002**, *29*, 2042. [[CrossRef](#)]
13. Zheng, X.B.; Kang, W.M.; Zhao, T.L. Long-term trends in sunshine duration over Yunnan-Guizhou Plateau in Southwest China for 1961–2005. *Geophys. Res. Lett.* **2008**, *35*, L15707. [[CrossRef](#)]
14. Carmichael, G.R.; Adhikary, B.; Kulkarni, S. Asian aerosols: Current and year 2030 distributions and implications to human health and regional climate change. *Environ. Sci. Technol.* **2009**, *43*, 5811–5817. [[CrossRef](#)] [[PubMed](#)]
15. Stanhill, G.A. perspective on global warming, dimming, and brightening. *Eos Trans. Am. Geophys. Union* **2007**, *88*, 58–59. [[CrossRef](#)]
16. Romanou, A.; Liepert, B.; Schmidt, G.A. 20th century changes in surface solar irradiance in simulations and observations. *Geophys. Res. Lett.* **2007**, *34*, 89–103. [[CrossRef](#)]
17. Wang, K.; Dickinson, R.E.; Liang, S. Clear sky visibility has decreased over land globally from 1973 to 2007. *Science* **2009**, *323*, 1468. [[CrossRef](#)]
18. Rosenfeld, D.; Dai, J.; Yu, X. Inverse relations between amounts of air pollution and orographic precipitation. *Science* **2007**, *315*, 1396–1398. [[CrossRef](#)]
19. Schütz, L.; Sebert, M. Mineral aerosols and source identification. *J. Aerosol Sci.* **1987**, *18*, 1–10. [[CrossRef](#)]
20. Huo, W.; Li, X.; Ai, L.; Wang, J.; Zhao, X.C. Analysis on the Features of Sandstorms in the Tarim Basin in Spring 2004. *Arid Zone Res.* **2004**, *2*, 210–215. (In Chinese) [[CrossRef](#)]
21. Tang, Y.; Han, Y.; Liu, Z. Temporal and spatial characteristics of dust devils and their contribution to the aerosol budget in East Asia—An analysis using a new parameterization scheme for dust devils. *Atmos. Environ.* **2018**, *182*, 225–233. [[CrossRef](#)]
22. Sattar, S.A.; Ijaz, M.K. Spread of viral infections by aerosols. *Crit. Rev. Environ. Control* **1987**, *17*, 89–131. [[CrossRef](#)]
23. Wake, B. Asian aerosol influence. *Nat. Clim. Change* **2012**, *2*, 487. [[CrossRef](#)]
24. Tian, X.M.; Tang, C.L.; Wu, X.; Yang, J.; Zhao, F.M.; Liu, D. The global spatial-temporal distribution and EOF analysis of AOD based on MODIS data during 2003–2021. *Atmos. Environ.* **2023**, *302*, 119722. [[CrossRef](#)]
25. Xu, X.; Qiu, J.; Xia, X.; Sun, L. Characteristics of atmospheric aerosol optical depth variation in China during 1993–2012. *Atmos. Environ.* **2015**, *119*, 82–94. [[CrossRef](#)]
26. He, Q.; Gu, Y.; Zhang, M. Spatiotemporal patterns of aerosol optical depth throughout China from 2003 to 2016. *Sci. Total Environ.* **2019**, *653*, 23–35. [[CrossRef](#)] [[PubMed](#)]
27. Liu, Y.; Lin, A.W.; Qin, W.M.; He, L.J.; Li, X. Spatial-temporal distribution of aerosol optical depth and its main influence types in China during 1990–2017. *Environ. Sci.* **2019**, *40*, 2572–2581. (In Chinese)
28. Kaufman, Y.J.; Joseph, J.H. Determination of surface albedos and aerosol extinction characteristics from satellite imagery. *J. Geophys. Res. Ocean.* **1982**, *87*, 1287–1299. [[CrossRef](#)]
29. Tanré, D.; Devaux, C.; Herman, M. Radiative properties of desert aerosols by optical ground-based measurements at solar wavelengths. *J. Geophys. Res. Atmos.* **1988**, *93*, 14223–14231. [[CrossRef](#)]
30. Holben, B.; Vermote, E.; Kaufman, Y.J. Aerosol retrieval over land from AVHRR data-application for atmospheric correction. *IEEE Trans. Geosci. Remote Sens.* **1992**, *30*, 212–222. [[CrossRef](#)]
31. Fraser, R.S.; Kaufman, Y.J.; Mahoney, R.L. Satellite measurements of aerosol mass and transport. *Atmos. Environ.* **1984**, *18*, 2577–2584. [[CrossRef](#)]
32. Durkee, P.A.; Jensen, D.R.; Hindman, E.E. The relationship between marine aerosol particles and satellite-detected radiance. *J. Geophys. Res. Atmos.* **1986**, *91*, 4063–4072. [[CrossRef](#)]
33. Tanré, D.; Legerand, M. On the satellite retrieval of Saharan dust optical thickness over land: Two different approaches. *J. Geophys. Res. Atmos.* **1991**, *96*, 5221–5227. [[CrossRef](#)]
34. Kaufman, Y.J.; Sendra, C. Algorithm for automatic atmospheric corrections to visible and near-IR satellite imagery. *Int. J. Remote Sens.* **1988**, *9*, 1357–1381. [[CrossRef](#)]
35. Kaufman, Y.J.; Tanré, D.; Gordon, H.R. Passive remote sensing of tropospheric aerosol and atmospheric correction for the aerosol effect. *J. Geophys. Res. Atmos.* **1997**, *102*, 16815–16830. [[CrossRef](#)]
36. Pozzer, A.; Meij, A.; Yoon, J.; Tost, H. AOD trends during 2001–2010 from observations and model simulations. *Atmos. Chem. Phys.* **2015**, *15*, 5521–5535. [[CrossRef](#)]
37. Chubarova, N.Y.; Poliukhov, A.A.; Gorlova, I.D. Long-term variability of aerosol optical thickness in Eastern Europe over 2001–2014 according to the measurements at the Moscow MSU MO AERONET site with additional cloud and NO₂ correction. *Atmos. Meas. Tech.* **2016**, *9*, 313–334. [[CrossRef](#)]

38. Li, C.C.; Mao, J.T.; Liu, Q.H. Using MODIS to study the distribution and seasonal variation of aerosol optical thickness in eastern China. *Chin. Sci. Bull.* **2003**, *48*, 2094–2100. (In Chinese) [[CrossRef](#)]
39. Zhang, Z.; Ding, J.L.; Wang, J.J. Regional Analysis of indirect effect of Aerosol in Arid area of Xinjiang. *China Environ. Sci.* **2016**, *36*, 3521–3530. (In Chinese)
40. Bai, B.; Zhang, Q.; Chen, X.H. Classification and characteristics of aerosols in arid and semi-arid regions of Northwest China. *J. Desert Res.* **2019**, *39*, 109–114. (In Chinese)
41. Zhang, L.; Jiang, H.; Chen, C. Temporal and spatial distribution of aerosol optical thickness of MODIS in Guangdong Province and its influencing factors. *Geospat. Inf.* **2017**, *15*, 46–49, 58. (In Chinese)
42. Xiang, Y.; Ye, Y.; Peng, C.C.; Teng, M.J.; Zhou, Z.X. Seasonal variations for combined effects of landscape metrics on land surface temperature (LST) and aerosol optical depth (AOD). *Ecol. Indic.* **2022**, *138*, 108810. [[CrossRef](#)]
43. Zhang, J.Y.; Lu, X.N.; Hong, J. Quantitative Study on Temporal and Spatial Patterns of Aerosol Optical Depth and Its Driving Forces in Sichuan Province during 2000–2014. *J. Nat. Resour.* **2016**, *31*, 1514–1525. (In Chinese)
44. Li, X.; Xia, X.G.; Wang, S.L. Validation of MODIS and Deep Blue aerosol optical depth retrievals in an arid/semi-arid region of northwest China. *Particuology* **2012**, *10*, 132–139. [[CrossRef](#)]
45. Wang, K.; Sun, X.; Zhou, Y.; Zhang, C. Validation of MODIS-Aqua Aerosol Products C051 and C006 over the Beijing-Tianjin-Hebei Region. *Atmosphere* **2017**, *8*, 172. [[CrossRef](#)]
46. Chen, Y.N.; Li, B.F.; Fan, Y.T. Hydrological and water cycle processes of inland river basins in the arid region of Northwest China. *J. Arid Land* **2019**, *11*, 161–179. [[CrossRef](#)]
47. Chen, D.T.; Liu, W.J.; Huang, F.R. Spatial-temporal characteristics and influencing factors of relative humidity in arid region of Northwest China during 1966–2017. *J. Arid Land* **2020**, *12*, 397–412. [[CrossRef](#)]
48. Wang, Y.J.; Qin, D.H. Influence of climate change and human activity on water resources in arid region of Northwest China: An overview. *Adv. Clim. Change Res.* **2017**, *8*, 268–278. [[CrossRef](#)]
49. Gupta, P.; Remer, L.A.; Patadia, F. High-Resolution Gridded Level 3 Aerosol Optical Depth Data from MODIS. *Remote Sens.* **2020**, *12*, 2847. [[CrossRef](#)]
50. Tao, M.H.; Chen, L.F.; Wang, Z.F. Evaluation of MODIS Deep Blue Aerosol Algorithm in Desert Region of East Asia: Ground Validation and Intercomparison. *J. Geophys. Res. Atmos.* **2017**, *122*, 10–357, 368. [[CrossRef](#)]
51. Yang, L.P.; Meng, X.M.; Zhang, X.Q. SRTM DEM and its application advances. *Int. J. Remote Sens.* **2011**, *32*, 3875–3896. [[CrossRef](#)]
52. Filonchik, M.; Yan, H.W.; Zhang, Z.R. Combined use of satellite and surface observations to study aerosol optical depth in different regions of China. *Sci. Rep.* **2019**, *9*, 6174. [[CrossRef](#)] [[PubMed](#)]
53. He, Q.Y.; Mu, F.Y.; Li, Q.Y.; Yang, M. Geography study on spatiotemporal evolution of fractional vegetation coverage and the driving forces in Chongqing. *Sci. Technol. Eng.* **2021**, *21*, 11955–11962. (In Chinese)
54. Yue, H.; Liu, Y.; Zhang, Y.M. Study on temporal and spatial variability of aerosol optical depth in China region based on MODIS data. *Environ. Pollut. Control* **2020**, *42*, 89–93. (In Chinese) [[CrossRef](#)]
55. Wang, Y.P.; Yu, X.; Xie, G.Q. Spatial distribution and temporal variation of aerosol optical depth over China in the past 15 years. *China Environ. Sci.* **2018**, *38*, 426–434. (In Chinese) [[CrossRef](#)]
56. Raj, P.E.; Devara, P.C.S.; Saha, S.K.; Dani, K.K.; Mahes Kumar, R.S. Spatio-temporal variations in aerosol properties over the Deccan Plateau region, India. *Pollut. Res.* **2009**, *28*, 547–553.
57. He, X.; Zhang, F.; Cai, Y.; Tan, M.L.; Chan, N.W. Spatio-temporal changes in fractional vegetation cover and the driving forces during 2001–2020 in the northern slopes of the Tianshan Mountains, China. *Environ. Sci. Pollut. Res.* **2023**, *30*, 75511–75531. [[CrossRef](#)]
58. Pearson, K. Notes on the history of correlation. *Biometrika* **1920**, *13*, 25–45. Available online: <https://www.jstor.org/stable/2331722> (accessed on 1 October 2023). [[CrossRef](#)]
59. Zhuang, H.M.; Zhang, C.; Cheng, F.; Zhang, L.L.; He, B.K. Spatiotemporal pattern of soil moisture and its meteorological driving factors in dry croplands across China from 1992 to 2018. *Acta Geogr. Sin.* **2022**, *77*, 2308–2321. (In Chinese)
60. Hu, T.; Xiao, C. Data-driven main color map feature learning, design and simulation for smart ethnic cloth. *Future Gener. Comput. Syst.* **2019**, *97*, 153–164. [[CrossRef](#)]
61. Abadi AR, S.; Hamzeh, N.H.; Shukurov, K.; Opp, C.; Dumka, U.C. Long-term investigation of aerosols in the Urmia Lake region in the Middle East by ground-based and satellite data in 2000–2021. *Remote Sens.* **2020**, *14*, 3827. [[CrossRef](#)]
62. Feng, H.; Zou, B.; Wang, J. Dominant variables of global air pollution-climate interaction: Geographic insight. *Ecol. Indic.* **2019**, *99*, 251–260. [[CrossRef](#)]
63. Andreae, M.O.; Rosenfeld, D. Aerosol–cloud–precipitation interactions. Part 1. The nature and sources of cloud-active aerosols. *Earth-Sci. Rev.* **2008**, *89*, 13–41. [[CrossRef](#)]
64. Qian, J.L.; Liu, C.S. Distributions and changes of aerosol optical depth on both sides of HU Huanyong Line and the response to land use and land cover. *Acta Sci. Circumstantiae* **2018**, *38*, 752–760. (In Chinese)
65. Namdari, S.; Karimi, N.; Sorooshian, A. Impacts of climate and synoptic fluctuations on dust storm activity over the Middle East. *Atmos. Environ.* **2018**, *173*, 265–276. [[CrossRef](#)] [[PubMed](#)]
66. Islam, M.M.; Mamun, M.M.I.; Islam, M.Z. Interactions of Aerosol Optical Depth and Cloud Parameters with Rainfall and the Validation of Satellite Based Rainfall Observations. *Am. J. Environ. Sci.* **2017**, *13*, 315–324. [[CrossRef](#)]

67. Feng, H.; Zou, B. Satellite-based separation of climatic and surface influences on global aerosol change. *Int. J. Remote Sens.* **2020**, *41*, 5443–5456. [[CrossRef](#)]
68. Abuelgasim, A.; Farahat, A. Effect of dust loadings, meteorological conditions, and local emissions on aerosol mixing and loading variability over highly urbanized semiarid countries: United Arab Emirates case study. *J. Atmos. Sol. -Terr. Phys.* **2020**, *199*, 105215. [[CrossRef](#)]
69. Han, D.W.; Liu, W.Q.; Zhang, Y.J. Influence of temperature and relative humidity upon aerosol mass concentrations vertical distributions. *J. Grad. Sch. Chin. Acad. Sci.* **2007**, *24*, 619–624. (In Chinese)
70. Latha, R.; Vinayak, B.; Murthy, B.S. Response of heterogeneous vegetation to aerosol radiative forcing over a northeast Indian station. *J. Environ. Manag.* **2018**, *206*, 1224–1232. [[CrossRef](#)]
71. Kergoat, L.; Guichard, F.; Pierre, C. Influence of dry-season vegetation variability on Sahelian dust during 2002–2015. *Geophys. Res. Lett.* **2017**, *44*, 5231–5239. [[CrossRef](#)]
72. Li, H.D.; Meier, F.; Lee, X.H. Interaction between urban heat island and urban pollution island during summer in Berlin. *Sci. Total Environ.* **2018**, *636*, 818–828. [[CrossRef](#)] [[PubMed](#)]
73. Zhang, L.L.; Pan, J.H.; Zhang, D.H. Spatio-temporal distribution characteristics of aerosol optical depths in China based on MODIS data. *Acta Sci. Circumstantiae* **2018**, *38*, 4431–4439. (In Chinese) [[CrossRef](#)]
74. Liu, J.; Ding, J.; Rexiding, M.; Li, X.; Zhang, J.; Ran, S.; Bao, Q.; Ge, X. Characteristics of dust aerosols and identification of dust sources in Xinjiang, China. *Atmos. Environ.* **2021**, *262*, 118651. [[CrossRef](#)]
75. Ren, G.; Pan, B.; Wang, J.; An, D.; Yang, M.; Liu, H. Spatiotemporal distribution of dust aerosol optical properties from CALIPSO and CATS observations in Xinjiang, China. *J. Atmos. Sol. -Terr. Phys.* **2023**, *243*, 106006. [[CrossRef](#)]
76. Zhang, Z.; Ding, J.L.; Wang, J.J. Temporal distribution of cloud and precipitation and their possible relationships with surface aerosols in Central Asia. *Acta Sci. Circumstantiae* **2017**, *37*, 61–72. (In Chinese) [[CrossRef](#)]
77. Guo, J.; Yin, Y.; Wang, Y.W. Numerical study of the dust distribution, source and sink, and transport features over East Asia. *China Environ. Sci.* **2017**, *37*, 801–812. (In Chinese)
78. Jing, Y.; Sun, Y.L.; Fu, H.C. Temporal and Spatial Variation of Aerosol Optical Depth and Analysis of influencing Factors in Beijing-Tianjin-Hebei Region from 2010 to 2016. *Environ. Sci. Technol.* **2018**, *41*, 110–119. (In Chinese)
79. Li, X.P.; Che, H.Z.; Wang, H. Spatial and temporal distribution of the cloud optical depth over China based on MODIS satellite data during 2003–2016. *J. Environ. Sci.* **2018**, *80*, 66–81. [[CrossRef](#)]
80. Zhu, Q.; Castellano, M.J.; Yang, G.S. Coupling soil water processes and nitrogen cycle across spatial scales: Potentials, bottlenecks and solutions. *Earth Sci. Rev.* **2018**, *187*, 248–258. [[CrossRef](#)]
81. Findell, K.L.; Berg, A.; Gentile, P. The impact of anthropogenic land use and land cover change on regional climate extremes. *Nat. Commun.* **2017**, *8*, 989. [[CrossRef](#)] [[PubMed](#)]

Disclaimer/Publisher’s Note: The statements, opinions and data contained in all publications are solely those of the individual author(s) and contributor(s) and not of MDPI and/or the editor(s). MDPI and/or the editor(s) disclaim responsibility for any injury to people or property resulting from any ideas, methods, instructions or products referred to in the content.